

# An Accurate Technique for Calculation of Radiation from Printed Reflectarrays

Min Zhou, Stig B. Sørensen, *Member, IEEE*, Erik Jørgensen, *Member, IEEE*, Peter Meincke, *Member, IEEE*, Oleksiy S. Kim, and Olav Breinbjerg, *Member, IEEE*

**Abstract**—The accuracy of various techniques for calculating the radiation from printed reflectarrays is examined and an improved technique based on the equivalent currents approach is proposed. The equivalent currents are found from a continuous plane wave spectrum calculated by use of the spectral dyadic Green’s function. This ensures a correct relation between the equivalent electric and magnetic currents and thus allows an accurate calculation of the radiation over the entire far-field sphere. A comparison with DTU-ESA Facility measurements of a reference offset reflectarray designed and manufactured specifically for this purpose is presented to demonstrate the accuracy of the proposed technique.

**Index Terms**—Reflectarray, accurate antenna analysis, antenna radiation pattern, method of moments (MoM), dyadic Green’s function, equivalent currents

## I. INTRODUCTION

PRINTED reflectarrays provide a way for realizing low-cost high-gain antennas for satellite applications and have been the subject of increasing research interest [1], [2]. In the analysis of printed reflectarrays, the main focus has been on the accurate determination of the currents on the array elements [3]–[5], while the calculation of the radiation pattern has received less attention. However, the latter is equally important, and for space applications where the accuracy demands are high, an accurate prediction of the radiation pattern is required and should not be neglected. Some of the few reported techniques in the literature include approximate formulas based on array element summations [6]–[8], stationary phase approximation of the spatial dyadic Green’s function (DGF) [9], and the field equivalence principle [5], [10]–[12]. The objective of this work is to compare different techniques for calculating the radiation from printed reflectarrays and to propose and validate an improved method.

The commonly adopted method for determining the currents is based on the spectral domain Method of Moments (SD-MoM). It assumes local periodicity such that the individual array element is embedded in an infinite array consisting of

identical elements [7]. This method is also used to determine the unknown currents on the array elements in this work.

This letter is organized as follows. Section II discusses the different techniques for radiation pattern calculation. The reference antenna is described in Section III. In Section IV, simulations are compared with the measured data, and conclusions are given in Section V.

The time factor  $e^{j\omega t}$  is assumed and suppressed throughout the letter.

## II. TECHNIQUES FOR CALCULATION OF RADIATION

Three techniques to calculate the radiation from printed reflectarrays will be considered in this letter and they will be described in this section.

### *Technique I: Stationary Phase Evaluation of DGF*

A simple technique to determine the radiation from printed reflectarrays is the direct calculation from the currents on the array elements using a spatial DGF assuming an infinite ground plane [9]. The spatial DGF is found through its spectral counterpart and expressed in terms of infinite integrals. The numerical evaluation of these integrals is computationally expensive [13]. However, for far-field radiation pattern calculations, the stationary phase approximation can be used [9].

The drawback of this technique is that the DGF assumes infinite substrate and ground plane, thus the finite substrate size is not taken into account and the radiation in the backward hemisphere cannot be determined.

### *Technique II: Equivalent Currents from Floquet Spectrum*

This technique utilizes the equivalent currents approach [14, p.106]. Equivalent currents are constructed on a surface enclosing the entire reflectarray. The currents are defined by

$$\mathbf{J}_S = \hat{n} \times \mathbf{H}, \quad \mathbf{M}_S = -\hat{n} \times \mathbf{E}, \quad (1)$$

where  $\mathbf{E}$  and  $\mathbf{H}$  are the total electric and magnetic fields at the surface and  $\hat{n}$  is the outward unit vector normal to the surface. Usually, the total field in the entire half space behind the reflectarray is assumed to be zero and the equivalent currents are computed only in the plane of the array elements. By placing a perfect electric or magnetic conductor behind this planar surface, the electric or magnetic current, respectively, is short-circuited. The image principle is then employed to double the magnetic or electric current [10], [11]. On the other hand, if both electric and magnetic currents are used,

Manuscript received July 11, 2011; revised August 19, 2011. The reflectarray antenna production and measurement is supported by the European Space Agency (ESTEC contract No.4000101041).

M. Zhou is with TICRA, Copenhagen, Denmark, and also with the Department of Electrical Engineering, Electromagnetic Systems, Technical University of Denmark, Kgs. Lyngby, Denmark (e-mail: mz@ticra.com)

S.B. Sørensen, E. Jørgensen and P. Meincke are with TICRA, Copenhagen, Denmark (e-mail: ticra@ticra.com)

O.S. Kim and O. Breinbjerg are with the Department of Electrical Engineering, Electromagnetic Systems, Technical University of Denmark, Kgs. Lyngby, Denmark (e-mail: osk@elektro.dtu.dk, ob@elektro.dtu.dk)

the radiation over the entire far-field sphere can be calculated. In this case, the equivalent currents on the back side and at the edges of the reflectarray are assumed to be zero [5].

The equivalent currents are determined through the Floquet space harmonics from the SDMOM formulation. Due to the periodicity, the equivalent currents for each array element is calculated only within its own unit cell, as illustrated in Fig. 1a. The equivalent currents for the  $i$ th and  $j$ th element are shown with solid and dashed lines, respectively. Thus, the contribution from each array element to the equivalent current is confined to its unit cell. By repeating this procedure for all array elements, equivalent currents on the surface,  $\mathcal{S}$ , covering all elements/unit cells are constructed. For practical reasons, the substrate and ground plane in reflectarrays are often extended at the edges, and the physical substrate size is then larger than  $\mathcal{S}$ . To correct for this, unit cells with no array elements are placed at the edges such that the extended substrate area  $\mathcal{S}_{\text{ext}}$  is also covered, see Fig. 2. In this way, equivalent currents on the entire surface  $\mathcal{S}_{\text{tot}} = \mathcal{S} + \mathcal{S}_{\text{ext}}$  are constructed.

It is sufficient to approximate the equivalent currents on each unit cell, using the fundamental Floquet space harmonic. This is valid since the distance between the array elements is usually selected to avoid grating lobes and all higher order Floquet space harmonics are thus evanescent waves that do not contribute to the far-field radiation. As a result, the equivalent currents are calculated assuming the electric and magnetic field on the unit cell surface being related through the plane wave relation. In addition, discontinuities in the equivalent currents are created due to the truncation of the currents at the border of each unit cell. These issues may result in erroneous radiation patterns, as will be shown in Section IV.

### Technique III: Equivalent Currents from Continuous Spectrum

We propose a novel technique combining the techniques I and II. This technique is based on the equivalent currents approach but these equivalent currents are calculated using a continuous spectrum formulation.

Like in techniques I and II, the currents on the array elements are calculated under the local periodicity assumption. The equivalent currents are constructed on a surface enclosing the entire reflectarray as given by (1). The total field on the back side and at the edges of the reflectarray are assumed to be zero. The tangential electric field at the plane of the array elements  $z = 0$  can be expanded in a spectrum of plane waves [15]

$$\mathbf{E}(x, y) = \frac{1}{4\pi^2} \iint_{-\infty}^{\infty} \mathcal{E}(k_x, k_y) e^{-j(k_x x + k_y y)} dk_x dk_y, \quad (2)$$

where the spectral amplitude  $\mathcal{E}(k_x, k_y)$  is

$$\mathcal{E}(k_x, k_y) = \tilde{\mathbf{G}}(k_x, k_y) \cdot \left( \tilde{\mathbf{J}}(k_x, k_y) - \mathbf{b}(k_x, k_y) \right). \quad (3)$$

Herein,  $\tilde{\mathbf{J}}(k_x, k_y)$  is the Fourier transformation of the electric current on the array elements and  $\mathbf{b}(k_x, k_y)$  is given by

$$\bar{\mathbf{b}}(k_x, k_y) = \frac{2}{\eta_0 k_0 \gamma_0} \begin{pmatrix} k_0^2 - k_y^2 & k_x k_y \\ k_x k_y & k_0^2 - k_x^2 \end{pmatrix} \cdot \mathcal{E}^i(k_x, k_y). \quad (4)$$

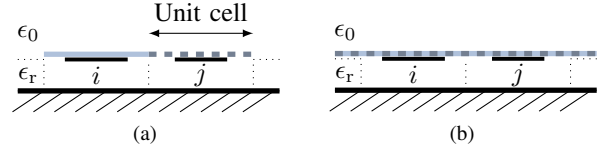


Fig. 1. Calculation of the equivalent currents for (a) technique II and (b) technique III. The equivalent currents for the  $i$ th and  $j$ th element is shown with solid and dashed lines, respectively.

In the above,  $\eta_0$  is the free space impedance,  $k_0$  the free space wavenumber, and  $\gamma_0 = \sqrt{k_0^2 - k_x^2 - k_y^2}$ . The quantity  $\mathcal{E}^i(k_x, k_y)$  is the spectral amplitude of the plane wave expansion of the incident electric field. The dyad  $\tilde{\mathbf{G}}(k_x, k_y)$  is the multilayer Green's function in the spectral domain. For the specific case of a single dielectric layer backed with an infinite ground plane, the terms in the spectral DGF can be found in [16, Eqs. (2)-(4)].

The numerical computation of (2) is cumbersome, but since only propagating waves contribute to the far-field radiation, the evanescent waves can be excluded in the integration to yield

$$\mathbf{E}(x, y) = \frac{1}{4\pi^2} \iint_{k_x^2 + k_y^2 < k_0^2} \mathcal{E}(k_x, k_y) e^{-j(k_x x + k_y y)} dk_x dk_y. \quad (5)$$

Consequently, the need of pole residue calculation or other cumbersome methods [17] can be avoided. The spectral integrals can be done in polar variables and performed efficiently using standard integration rules. Once  $\mathcal{E}(k_x, k_y)$  is determined, the magnetic field can be readily obtained using the plane wave relation

$$\mathbf{H}(x, y) = \frac{1}{4\pi^2} \iint_{k_x^2 + k_y^2 < k_0^2} \frac{1}{\eta_0} \hat{\mathbf{k}} \times \mathcal{E}(k_x, k_y) \cdot e^{-j(k_x x + k_y y)} dk_x dk_y, \quad (6)$$

where  $\hat{\mathbf{k}} = \hat{x}k_x + \hat{y}k_y \pm \hat{z}\gamma_0$  describes the direction of propagation. Upon substitution in (1), the equivalent currents are calculated over the entire surface  $\mathcal{S}_{\text{tot}}$ , thus automatically accounting for the area  $\mathcal{S}_{\text{ext}}$ . A graphical illustration is shown in Fig. 1b, where the equivalent currents for the  $i$ th and  $j$ th element are again shown with solid and dashed lines, respectively. The currents cover the entire  $\mathcal{S}_{\text{tot}}$ , and the contribution from each array element over the entire surface is taken into account. Contrary to technique II, the electric and magnetic field at the reflectarray surface are related through the continuous plane wave spectrum and not through the plane wave relation of the fundamental Floquet space harmonic.

An overhead associated with the numerical evaluation of (5)-(6) do not significantly increase the overall computation time. For the reflectarray to be described in Section III, the computation times for techniques I, II and III using a 2.8 GHz Intel processor laptop are 25, 28 and 30 seconds, respectively.

### III. REFERENCE ANTENNA

The reflectarray antenna first reported in [5] is used as reference and its geometrical parameters are summarized in Table I. The antenna is designed to exaggerate the lack of

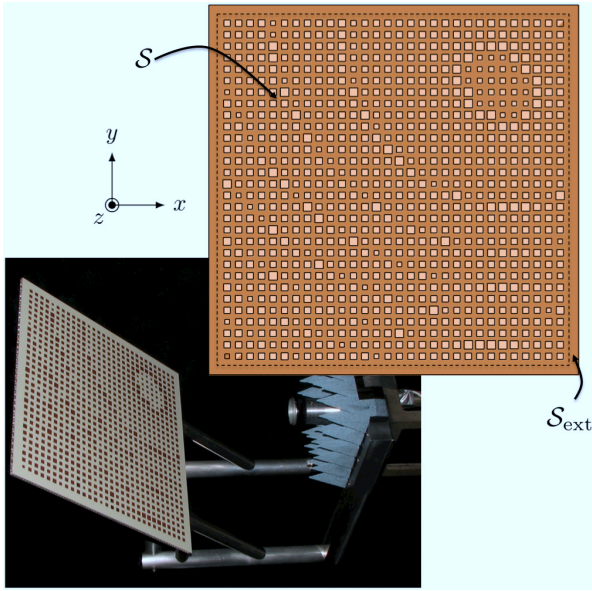


Fig. 2. Reflectarray designed with a pencil beam directed towards  $\theta = 35^\circ$  and  $\phi = 135^\circ$  in the shown coordinate system, and measured at the DTU-ESA Spherical Near-Field Antenna Test Facility. The surface  $\mathcal{S}$  is the area confined within the dashed lines covering the unit cells, and  $\mathcal{S}_{\text{ext}}$  covers the extended substrate area.

periodicity by having a pencil beam towards  $\theta = 35^\circ$  and  $\phi = 135^\circ$  in the coordinate system shown in Fig. 2. The feed is an  $x$ -polarized Potter horn with a 3 dB beamwidth of  $40^\circ$ , yielding an edge illumination varying from approximately  $-20$  to  $-5$  dB. The reflectarray and its support structures are manufactured at the Technical University of Denmark (DTU) and measured at the DTU-ESA-Spherical Near-Field Antenna Test Facility [18]. For the peak directivity, the measurements have a  $1\sigma$  uncertainty of 0.07 dB. The measured gain of the reflectarray is 28.74 dB. In addition to the reflectarray measurements, the Potter horn is also measured and the measured data are used in the SDMOM calculations.

#### IV. SIMULATIONS VS. MEASUREMENTS

The radiation patterns at 9.6 GHz obtained by measurements and simulations using techniques I-III are shown in Fig. 3. To account for the presence of the support structures, the scattering from the struts is included in the analysis using the MoM add-on in GRASP [19]. For techniques II and III both electric and magnetic currents are used. Results using only electric or magnetic currents are not shown since they yield patterns similar to those obtained using both currents but limited to the forward hemisphere.

All three techniques are capable of determining the main beam direction and beamwidth with good accuracy. However, technique I is very inaccurate in predicting the side lobes since the finite substrate size is not accounted for. Techniques II and III on the other hand accounts for the finite substrate size and therefore yield patterns that are in good agreement with the measurements. The peak directivity is measured to  $D_{\text{meas}} = 29.35$  dB. Techniques I and II yield  $D_{\text{I}} = 29.11$  dB and  $D_{\text{II}} = 29.10$  dB, respectively, whereas technique III gives an improved value of  $D_{\text{III}} = 29.30$  dB.

TABLE I  
REFERENCE REFLECTARRAY DATA

Frequency	9.6 GHz
Number of elements	$30 \times 30$
Reflectarray dimensions	435 mm $\times$ 435 mm
Substrate thickness	0.762 mm
Relative permittivity ( $\epsilon_r$ )	3.66
Loss tangent ( $\tan \delta$ )	0.0037
Feed distance to center of array	0.35 m
Feed offset angle	$\theta = 45^\circ, \phi = 0^\circ$
Main beam direction	$\theta = 35^\circ, \phi = 135^\circ$

To illustrate the accuracy in the back hemisphere, the radiation in the entire sphere is shown in Fig. 4. The agreement with the measurement is good for both techniques II and III. However, it is seen that in the direction of the main beam's image around  $\theta = 145^\circ$  and  $\phi = 135^\circ$ , technique II gives an erroneous beam, both for the co-polar and the cross-polar component. Usually, the equivalent electric and magnetic currents each gives strong contributions in the direction of the image, but in sum they cancel each other. Thus, such an erroneous beam should not exist if the currents are correctly related. There are several error sources that can introduce such an incorrect relation as described in the following.

In technique II, the equivalent currents are calculated under the approximation that the electric and magnetic fields in each unit cell are related by the plane wave relation. This approximation is inaccurate for configurations where the reflectarray is located close to the feed. Thus, errors are introduced in the equivalent currents resulting in an incorrect relation between them. In addition, the total equivalent currents are composed of truncated currents, and jumps in phase and amplitude can occur at the borders of the unit cells. This can give phase and amplitude errors, especially for aperiodic reflectarrays, and thus further deteriorating the relation between the equivalent currents. These sources of error give an incorrect relation between the equivalent currents and thus causing the erroneous beam. For reflectarrays made of slowly varying-sized elements

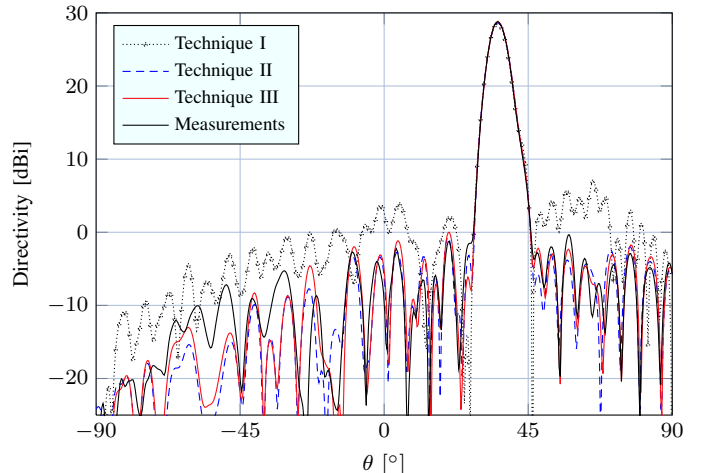


Fig. 3. Simulated and measured radiation patterns of the co-polar component at  $\phi = 135^\circ$ . Both electric and magnetic currents are used in techniques II and III.

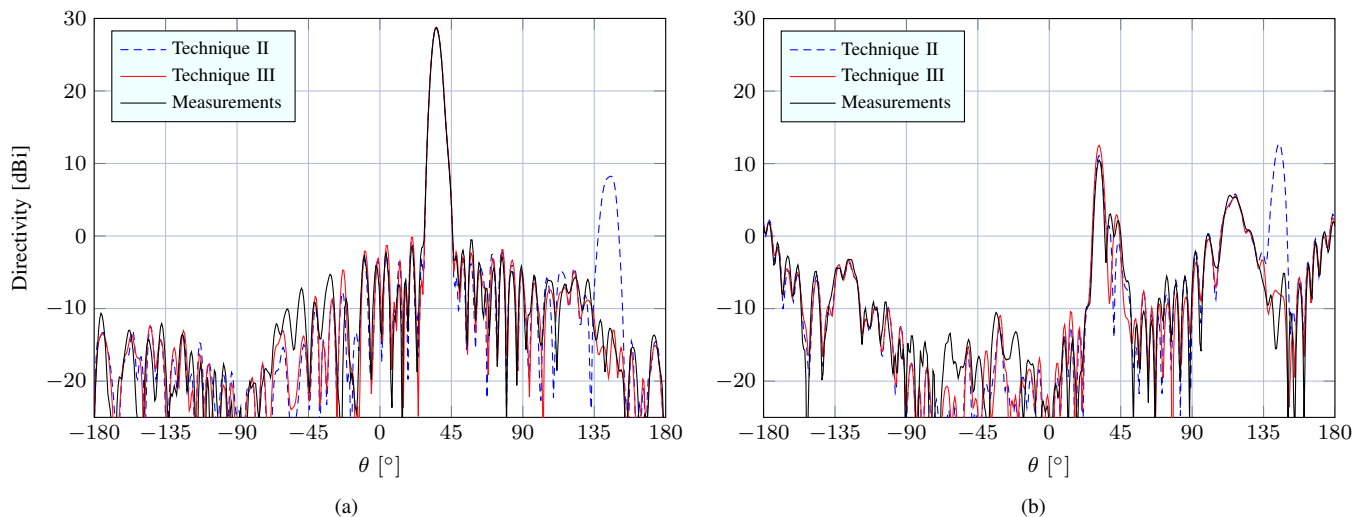


Fig. 4. Simulated and measured radiation patterns of the (a) co-polar and (b) cross-polar components at  $\phi = 135^\circ$ .

and with large feed distances, the errors diminish and no erroneous beams are created.

This problem is circumvented in technique III. No discontinuities are created in the equivalent currents, and the electric and magnetic currents are correctly related through the continuous plane wave spectrum. Hence the sum of the two gives an accurate pattern in the entire far-field sphere. The remaining discrepancies seen in Fig. 3 and Fig. 4 are mainly attributed to the local periodicity approximation in the SDMoM analysis [5].

## V. CONCLUSION

Several techniques to calculate the radiation from printed reflectarrays have been compared and an improved technique based on the equivalent currents approach has been proposed. The equivalent currents are determined from a continuous plane wave spectrum computed using the spectral dyadic Green's function. This ensures the correct relation between the equivalent electric and magnetic currents and enables an accurate calculation of the radiation over the entire sphere. An offset reflectarray has been manufactured and measured to serve as reference. Comparisons of simulated and measured radiation patterns show that the choice of the technique to calculate the radiation is very important with respect to the analysis accuracy. The finite substrate and ground plane size of the reflectarray must be accounted for and techniques that neglect this yield inaccurate radiation patterns. The comparisons also show that the proposed technique improves the accuracy of calculating the radiation from printed reflectarrays.

## ACKNOWLEDGMENT

Dr. Sergey Pivnenko, DTU, is acknowledged for the high-accuracy measurements of the reflectarray samples.

## REFERENCES

- [1] J. Huang and J. A. Encinar, *Reflectarray Antennas*. IEEE Press, 2008.
- [2] J. A. Encinar, "Recent advances in reflectarray antennas," in *Proc. EuCAP 2010*, Barcelona, Spain, 2010.
- [3] M. A. Milon, D. Cadoret, R. Gillard, and H. Legay, "Surrounded-element approach for the simulation of reflectarray radiating cells," *IET Microw. Antennas Propag.*, vol. 1, no. 2, pp. 289–293, 2007.
- [4] M. Arrebola, Y. Alvarez, J. A. Encinar, and F. Las-Heras, "Accurate analysis of printed reflectarrays considering the near field of the primary feed," *IET Microw. Antennas Propag.*, vol. 3, no. 2, pp. 187–194, 2009.
- [5] M. Zhou, S. B. Sørensen, E. Jørgensen, P. Meincke, O. S. Kim, and O. Breinbjerg, "Analysis of printed reflectarrays using extended local periodicity," in *Proc. EuCAP 2011*, Rome, Italy, 2011.
- [6] D. C. Chang and M. C. Huang, "Multiple-polarization microstrip reflectarray antenna with high efficiency and low cross-polarization," *IEEE Trans. Antennas Propag.*, vol. 43, no. 8, pp. 829–834, 1995.
- [7] D. M. Pozar, S. D. Targonski, and H. D. Syrigos, "Design of millimeter wave microstrip reflectarrays," *IEEE Trans. Antennas Propag.*, vol. 45, no. 2, pp. 287–296, 1997.
- [8] A. W. Robinson, M. E. Bialkowski, and H. J. Song, "A passive reflect array with dual-feed microstrip patch elements," *Microwave Opt. Technol. Lett.*, vol. 23, no. 5, pp. 295–299, 1999.
- [9] D. M. Pozar, "Radiation and scattering from a microstrip patch on a uniaxial substrate," *IEEE Trans. Antennas Propag.*, vol. 35, no. 6, pp. 613–621, 1987.
- [10] S. R. Rengarajan, "Reciprocity considerations in microstrip reflectarrays," *IEEE Antennas Wireless Propag. Lett.*, vol. 8, pp. 1206–1209, 2009.
- [11] M. Arrebola, J. A. Encinar, and M. Barba, "Multifed printed reflectarray with three simultaneous shaped beams for LMDS central station antenna," *IEEE Trans. Antennas Propag.*, vol. 56, no. 6, pp. 1518–1527, 2008.
- [12] H. Li, B.-Z. Wang, L. Guo, W. Shao, and P. Du, "A far field pattern analysis technique for reflectarrays including mutual coupling between elements," *J. Electromag. Waves Appl.*, vol. 23, pp. 87–95, 2009.
- [13] K. Michalski and J. R. Mosig, "Multilayered media Green's functions in integral equation formulations," *IEEE Trans. Antennas Propag.*, vol. 45, no. 3, pp. 508–519, 1997.
- [14] R. F. Harrington, *Time-Harmonic Electromagnetic Fields*. McGraw-Hill, Inc., 1961.
- [15] G. Kristensson, S. Poulsen, and S. Rikte, "Propagators and scattering of electromagnetic waves in planar bianisotropic slabs - an application to frequency selective structures," *Progr. Electromagn. Res. (PIER)*, pp. 1–25, 2004.
- [16] D. Pozar and D. Schaubert, "Analysis of an infinite array of rectangular microstrip patches with idealized probe feeds," *IEEE Trans. Antennas Propag.*, vol. 32, no. 10, pp. 1101–1107, 1984.
- [17] Y. Chow, J. Yang, D. Fang, and G. Howard, "A closed-form spatial Green's function for the thick microstrip substrate," *IEEE Trans. Microwave Theory Tech.*, vol. 39, no. 3, pp. 588–592, 1991.
- [18] "DTU-ESA Spherical Near-Field Antenna Test Facility." [Online]. Available: <http://www.dtu.dk/centre/ems/English/research/facilities.aspx>
- [19] K. Pontoppidan, Ed., *GRASP9, Technical Description*. TICRA Engineering Consultants, 2008.